Anticancer potential of copper(I) complexes based on isopropyl ester derivatives of bis(pyrazol-1-yl)acetate ligands

Maura Pellei,[a] Carlo Santini,[a*] Miriam Caviglia,[a] Jo' Del Gobbo,[a] Chiara Battocchio,[b] Carlo Meneghini,[b] Simone Amatori,[b] Chiara Donati,[c] Eleonora Zampieri,[c] Valentina Gandin[c*] Cristina Marzano,[c]

[a]*School of Science and Technology, Chemistry Division, University of Camerino, via Madonna delle Carceri (ChIP), 62032 Camerino, Italy*

[b]*Department of Science, Roma Tre University, Via della Vasca Navale 79, 00146 Roma, Italy*

[c]*Department of Pharmaceutical and Pharmacological Sciences, University of Padova, via Marzolo 5, 35131 Padova, Italy*

*****Correspondence: carlo.santini@unicam.it; valentina.gandin@unipd.it;

Supplementary material

Table of Contents:

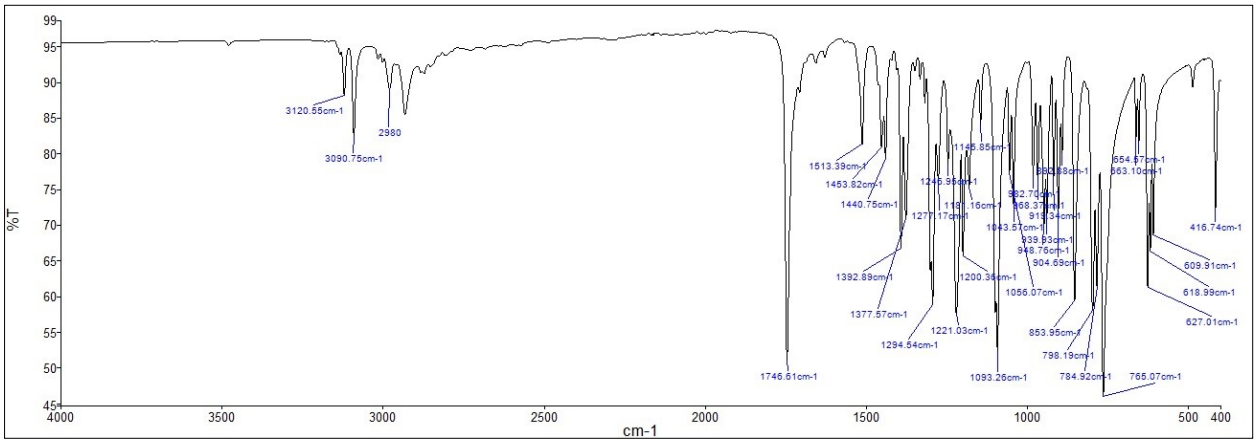

Figure S1. FT-IR spectrum of $HC(pz)_2COO^iPr$ (L^{OiPr}).

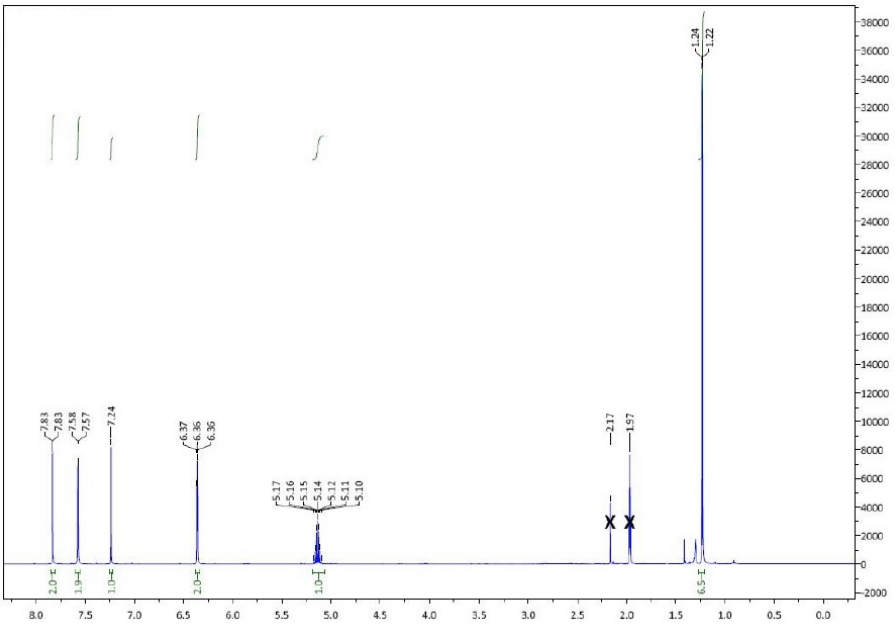

Figure S2. ^{1}H-NMR spectrum of $HC(pz)_2COO^iPr$ (L^{OiPr}) in CD_3CN.

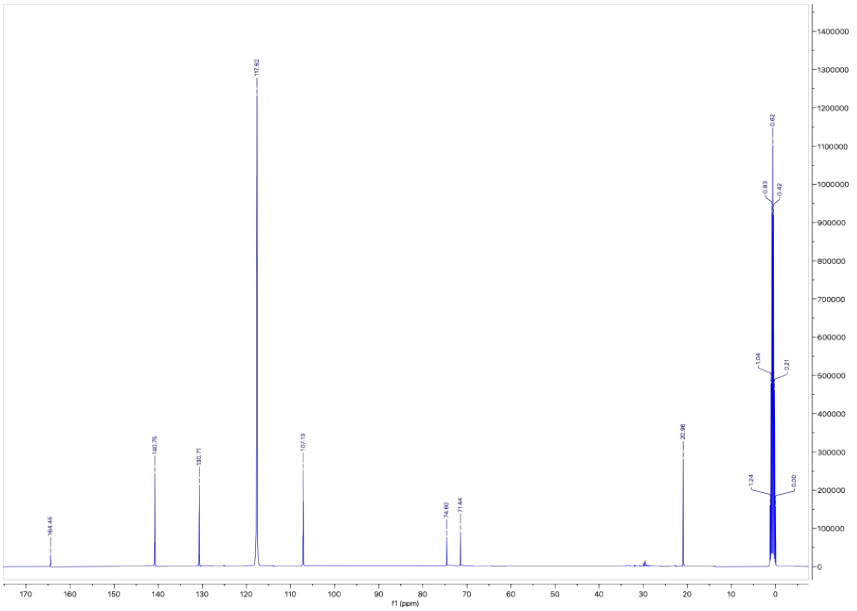

Figure S3. $^{13}C\{^{1}H\}$-NMR spectrum of $HC(pz)_2COO^iPr$ (L^{OiPr}) in CD_3CN.

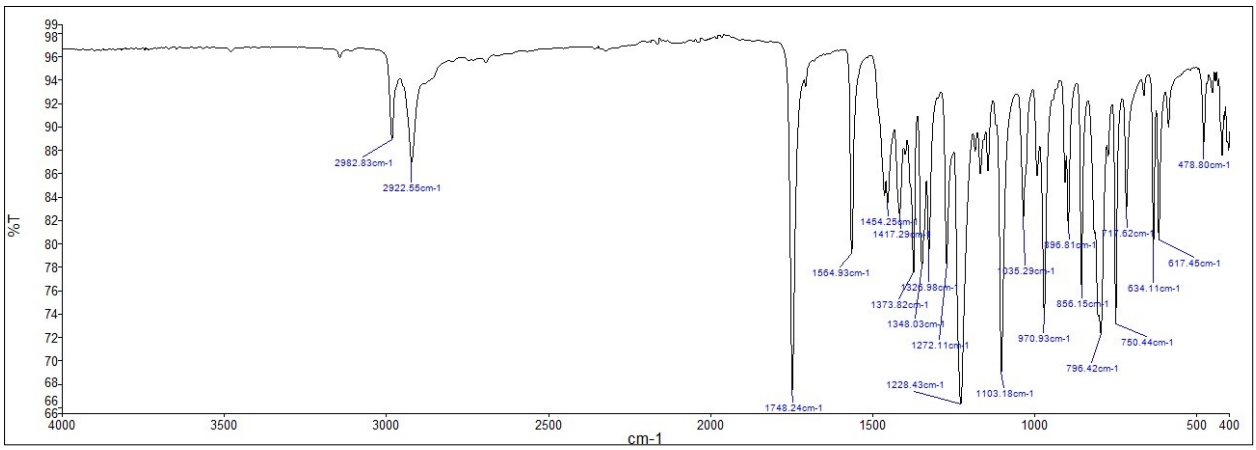

Figure S4. FT-IR spectrum of $HC(3,5\text{-}Me_2pz)_2CH(COO^iPr)$ (L^{2OiPr}).

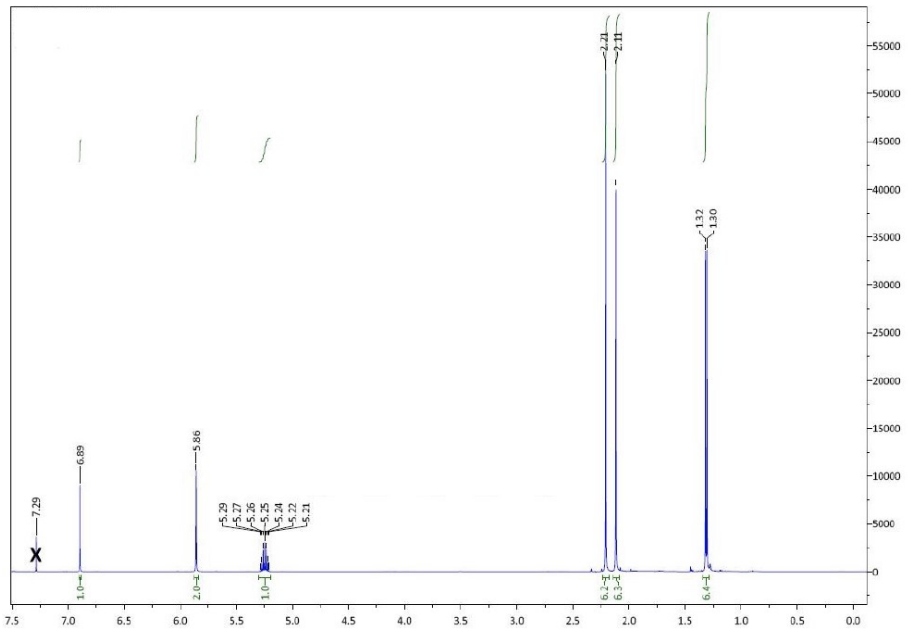

Figure S5. ^{1}H-NMR spectrum of HC(3,5-Me_2pz)$_2$CH(COO^{i}Pr) (L^{2OiPr}) in $CDCl_3$.

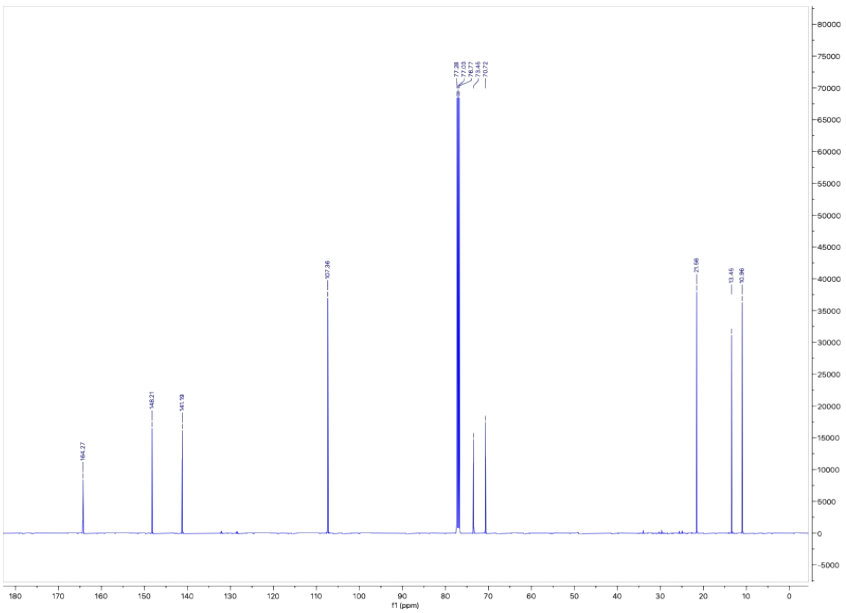

Figure S6. ^{13}C{^{1}H}-NMR spectrum of HC(3,5-Me_2pz)$_2$CH(COO^{i}Pr) (L^{2OiPr}) in $CDCl_3$.

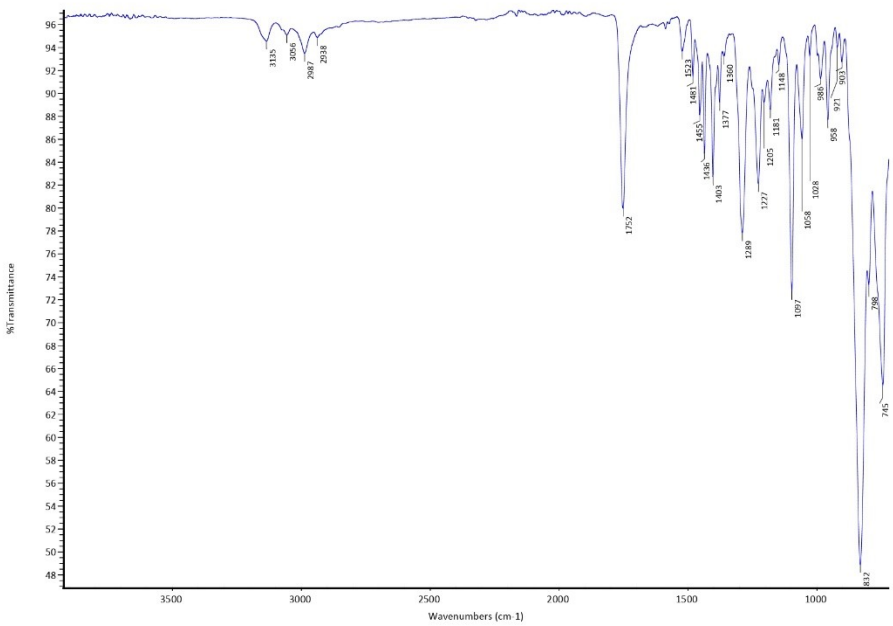

Figure S7. FT-IR spectrum of $[Cu(L^{OiPr})(PPh_3)]PF_6$ (**1**).

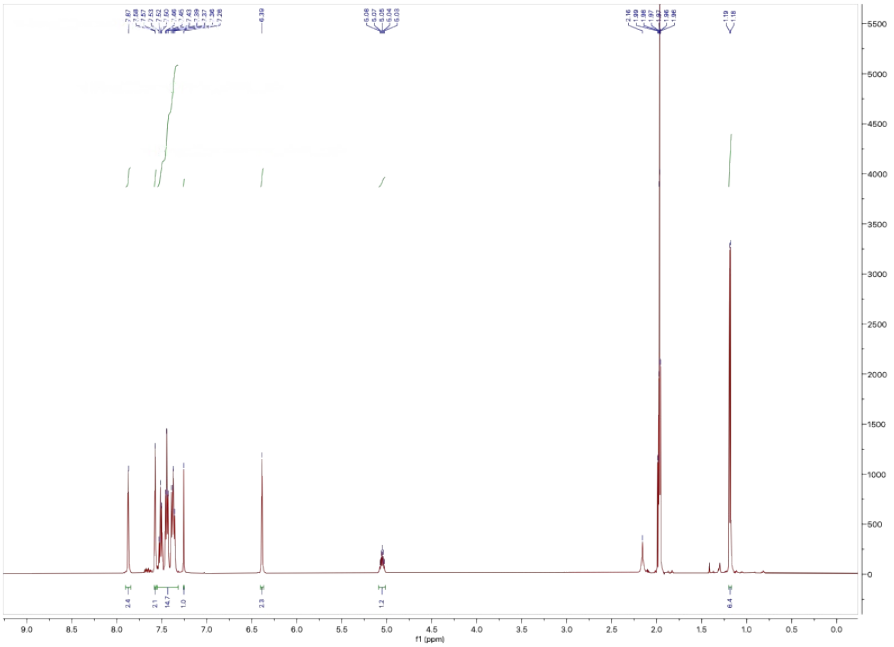

Figure S8. ^{1}H-NMR spectrum of $[Cu(L^{OiPr})(PPh_3)]PF_6$ (**1**) in CD_3CN.

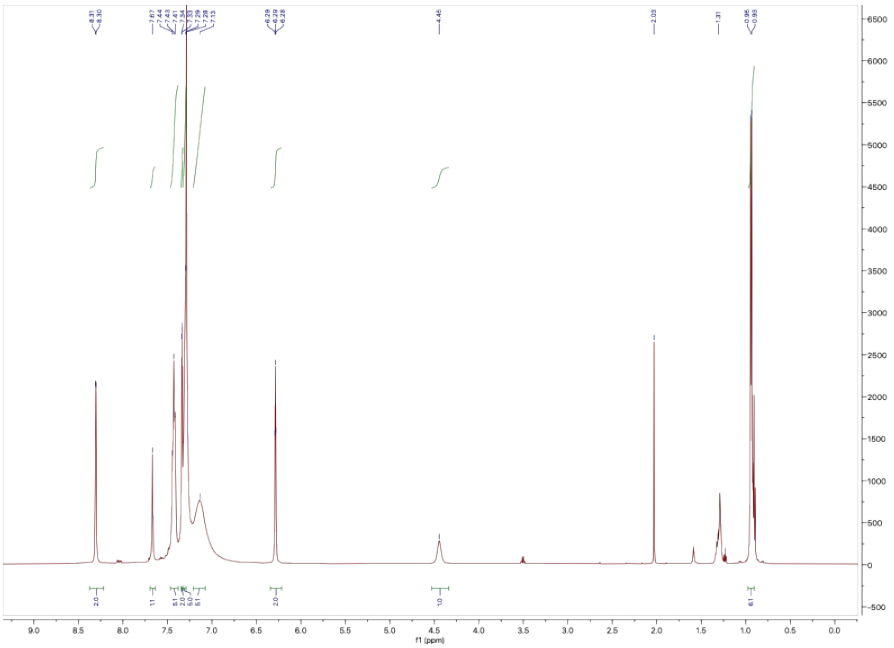

Figure S9. ^{1}H-NMR spectrum of [Cu(L^{OiPr})(PPh_3)]PF_6 (**1**) in $CDCl_3$.

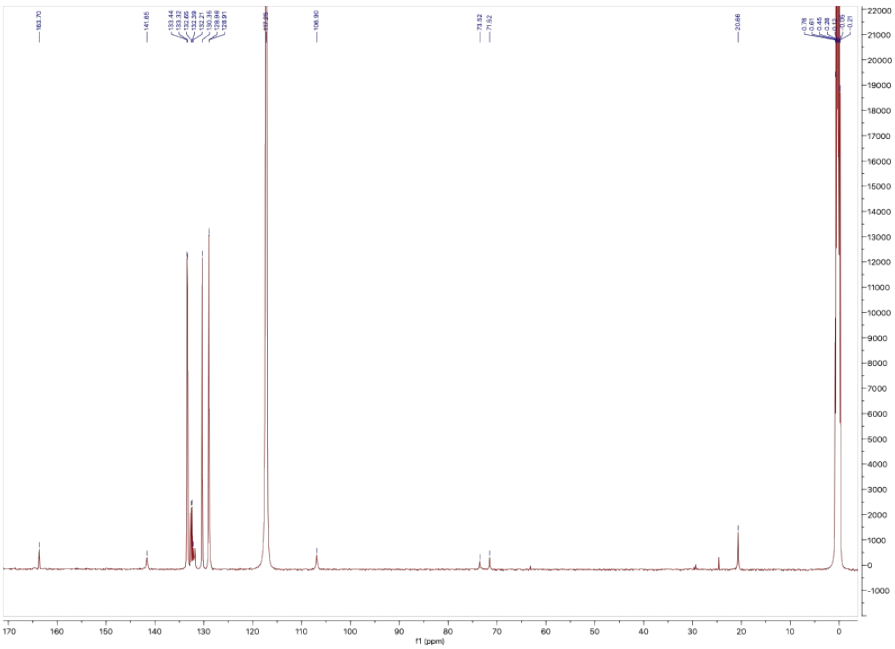

Figure S10. $^{13}C\{^{1}H\}$-NMR spectrum of [Cu(L^{OiPr})(PPh_3)]PF_6 (**1**) in CD_3CN.

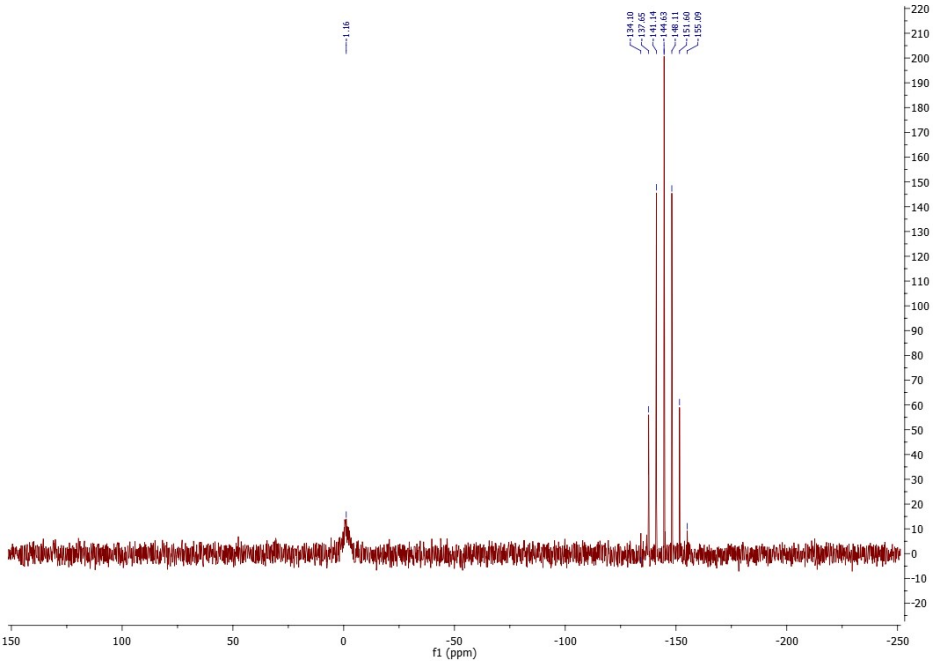

Figure S11. $^{31}P\{^{1}H\}$-NMR spectrum of $[Cu(L^{OiPr})(PPh_3)]PF_6$ (**1**) in CD_3CN at 293K.

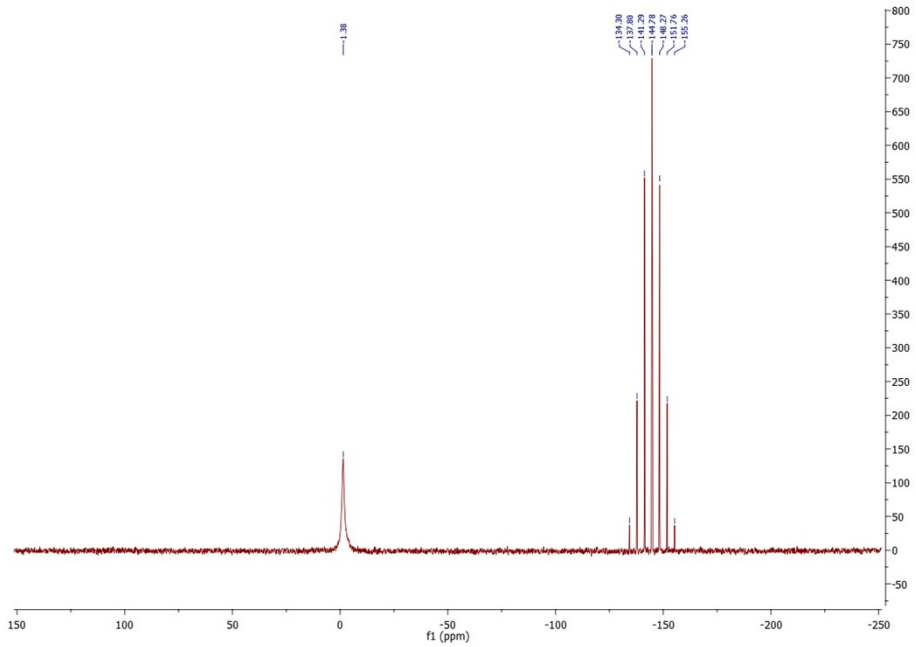

Figure S12. $^{31}P\{^{1}H\}$-NMR spectrum of $[Cu(L^{OiPr})(PPh_3)]PF_6$ (**1**) in CD_3CN at 243K.

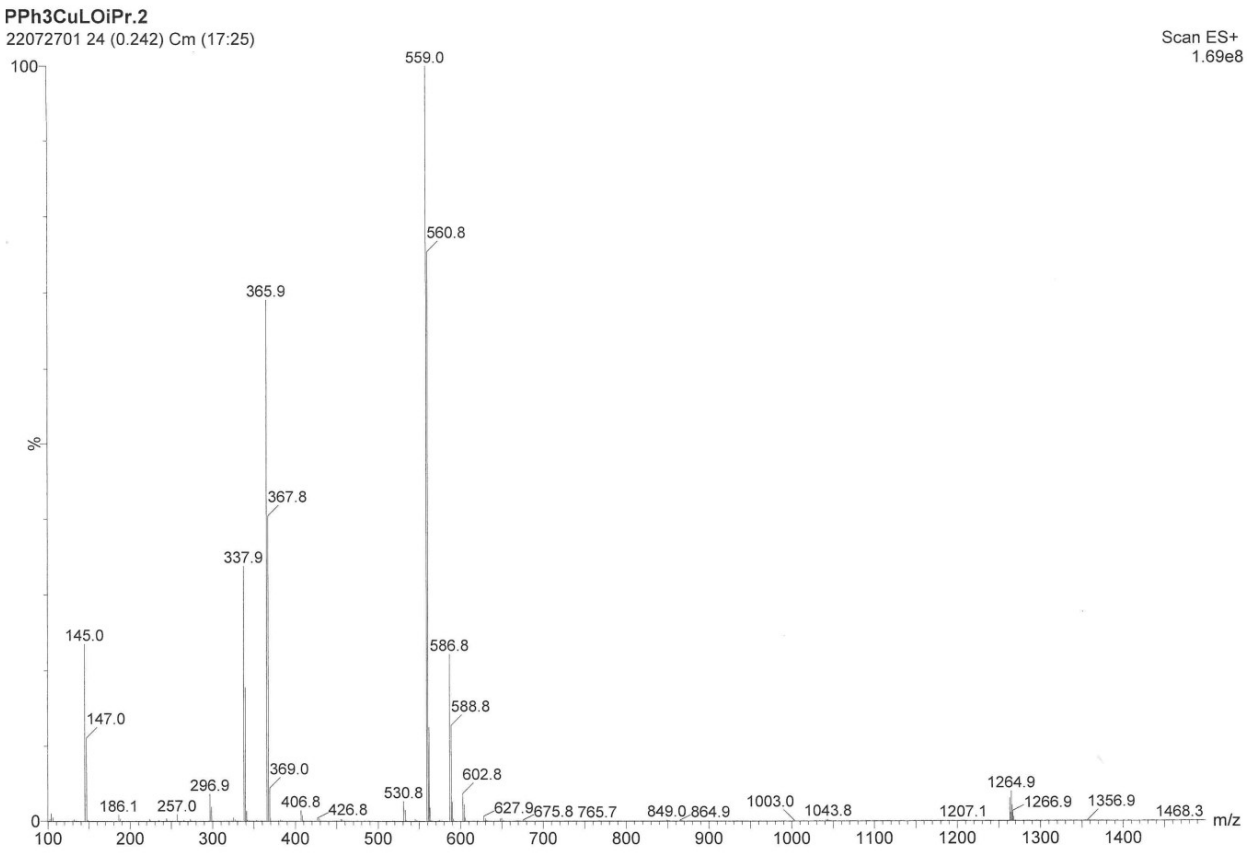

Figure S13. ESI-MS(+) spectrum in CH_3CN of $[Cu(L^{OiPr})(PPh_3)]PF_6$ (**1**).

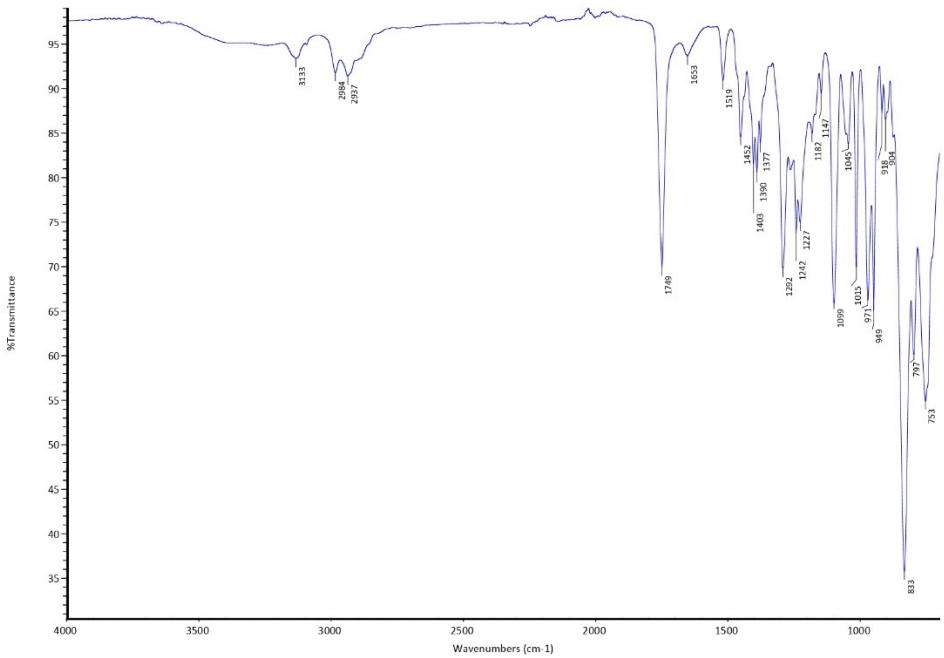

Figure S14. FT-IR spectrum of $[Cu(L^{OiPr})(PTA)]PF_6$ (**2**).

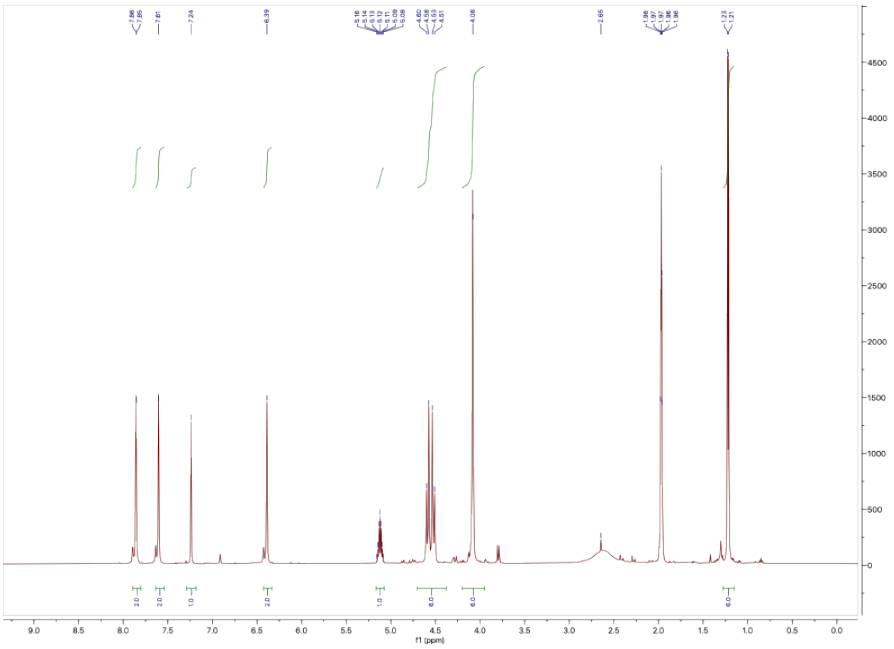

Figure S15. ^{1}H-NMR spectrum of [Cu(L^{OiPr})(PTA)]PF_6 (**2**) in CD_3CN.

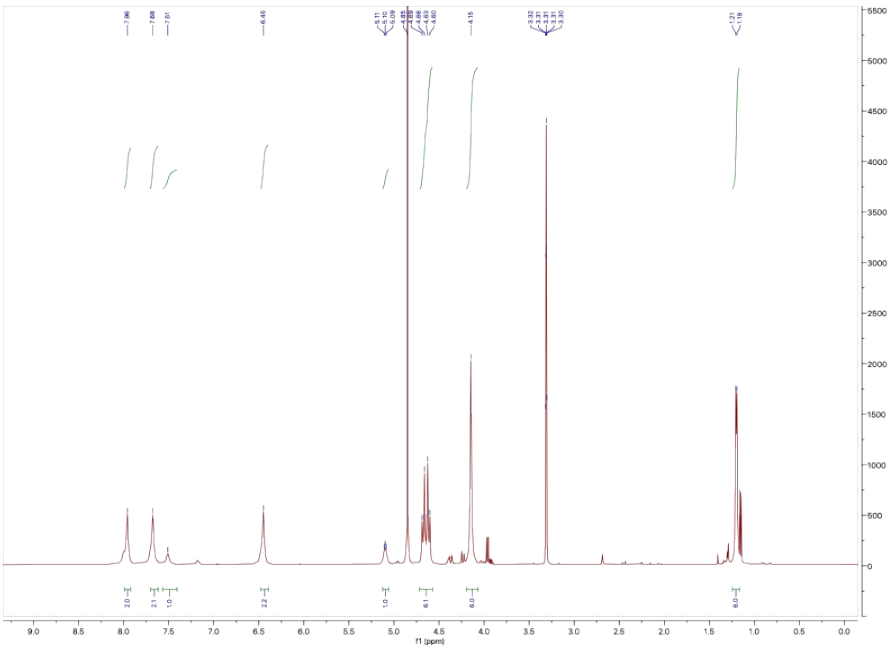

Figure S16. ^{1}H-NMR spectrum of [Cu(L^{OiPr})(PTA)]PF_6 (**2**) in CD_3OD.

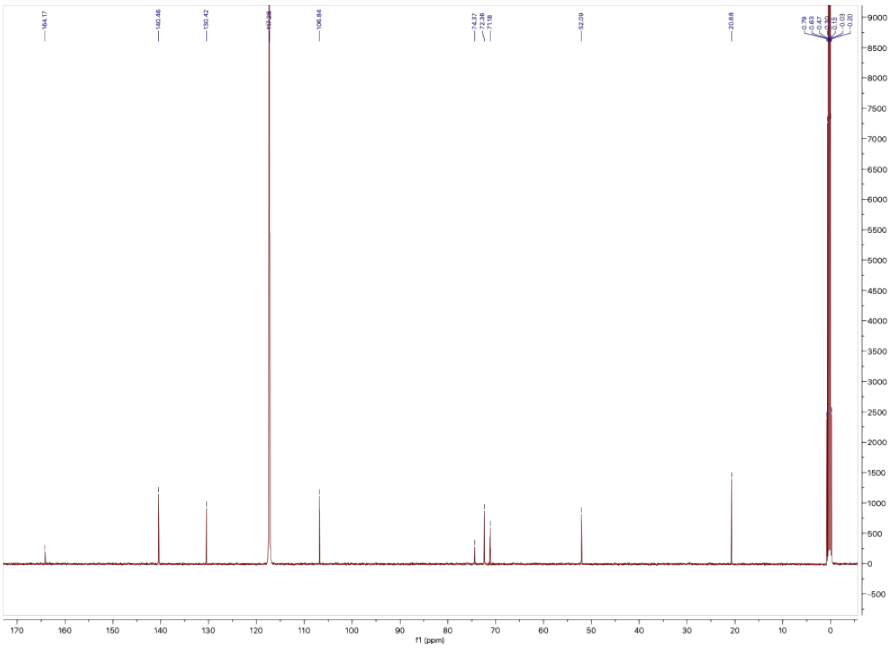

Figure S17. $^{13}C\{^{1}H\}$-NMR spectrum of $[Cu(L^{OiPr})(PTA)]PF_6$ (**2**) in CD_3CN.

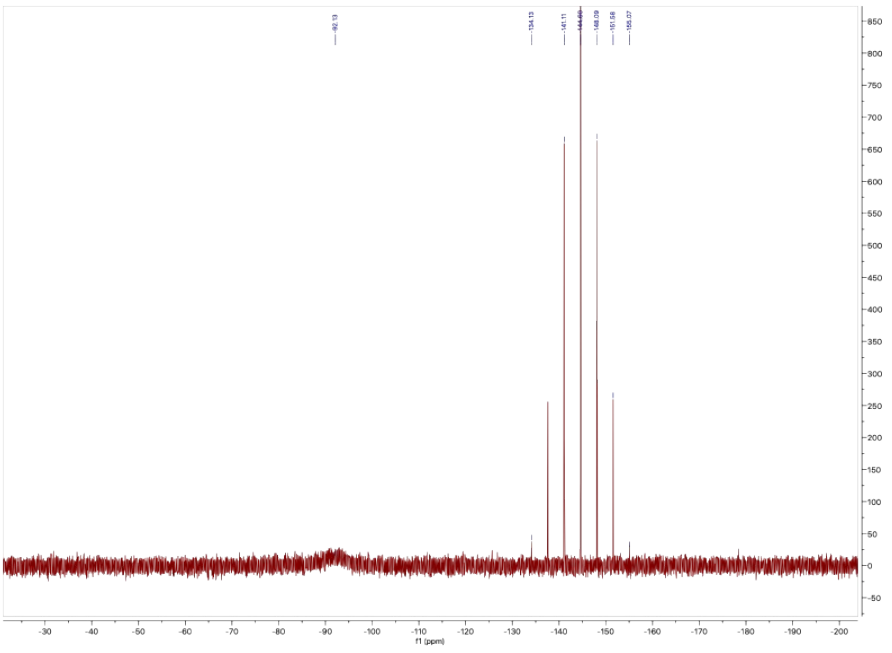

Figure S18. $^{31}P\{^{1}H\}$-NMR spectrum of $[Cu(L^{OiPr})(PTA)]PF_6$ (**2**) in CD_3CN at 293K.

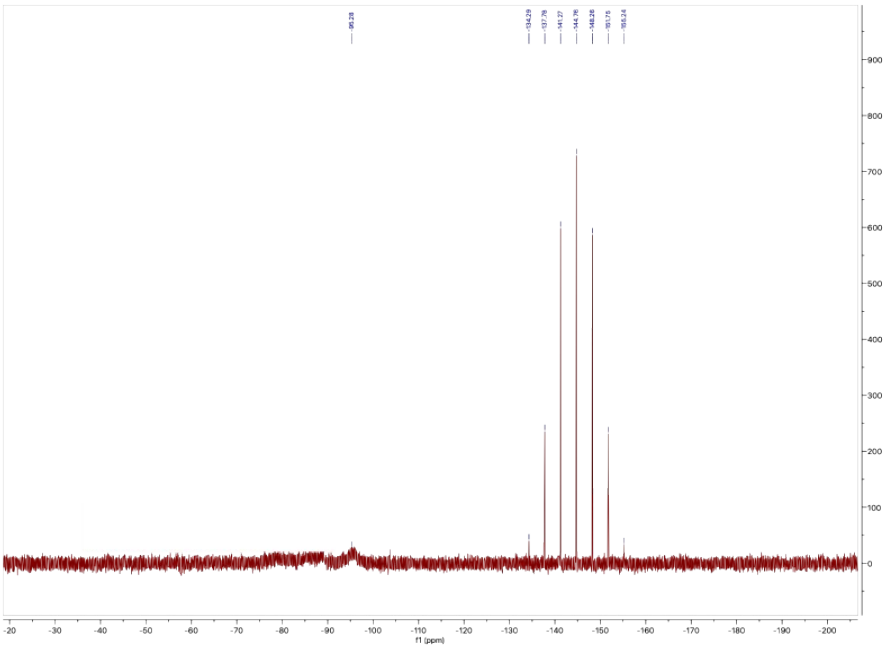

Figure S19. $^{31}P\{^{1}H\}$-NMR spectrum of [Cu(L^{OiPr})(PTA)]PF_6 (**2**) in CD_3CN at 243K.

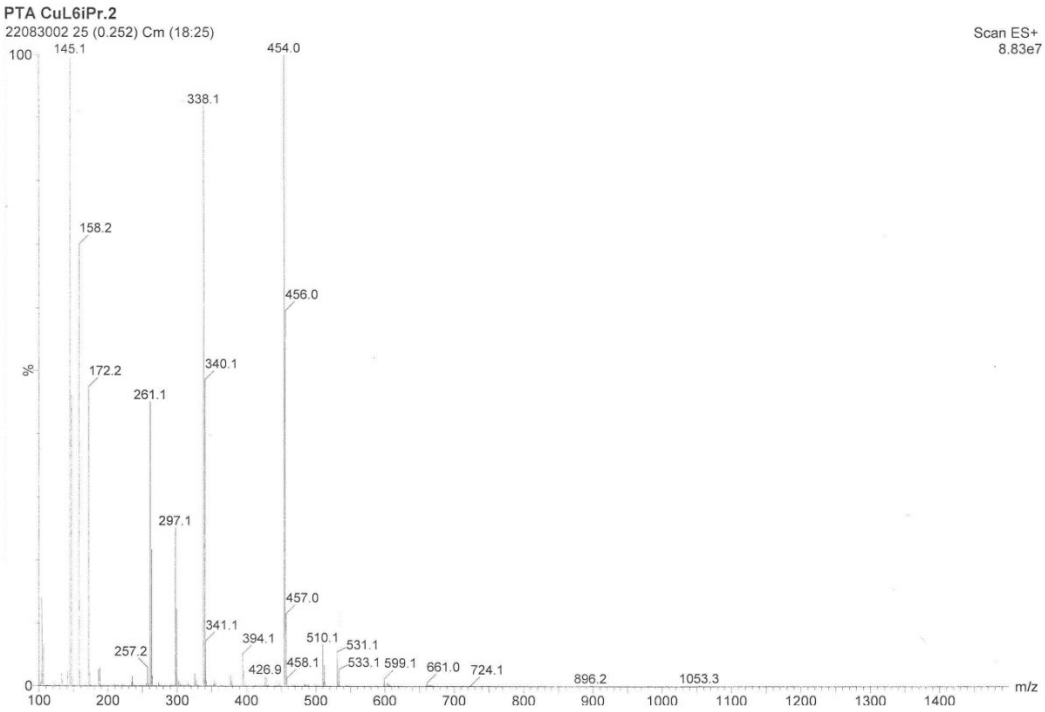

Figure S20. ESI-MS(+) spectrum in CH_3CN of [Cu(L^{OiPr})(PTA)]PF_6 (**2**).

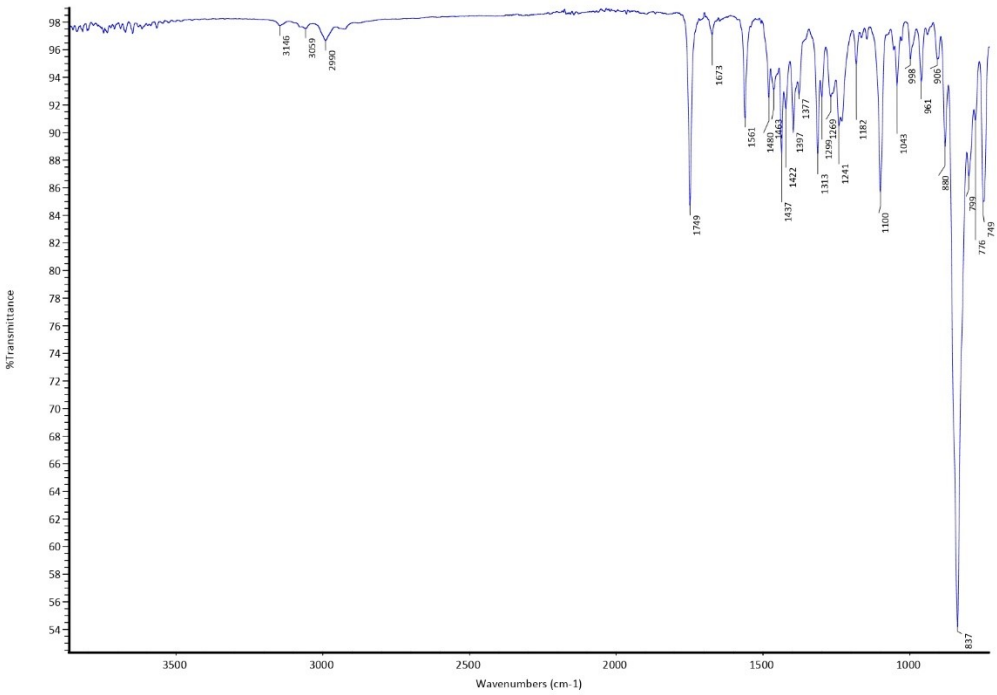

Figure S21. FT-IR spectrum of $[Cu(L^{2OiPr})(PPh_3)]PF_6$ (**3**).

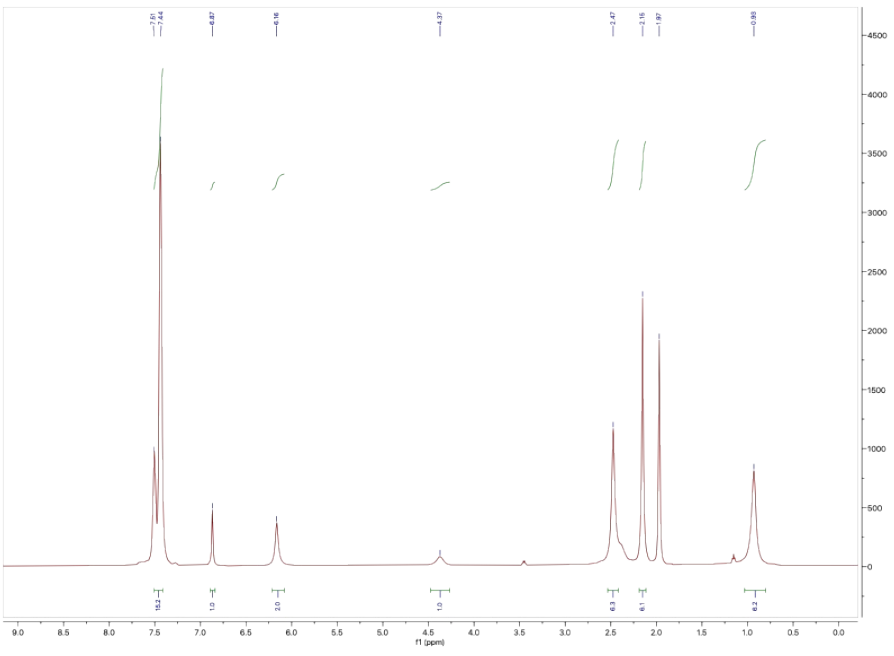

Figure S22. ^{1}H-NMR spectrum of $[Cu(L^{2OiPr})(PPh_3)]PF_6$ (**3**) in CD_3CN.

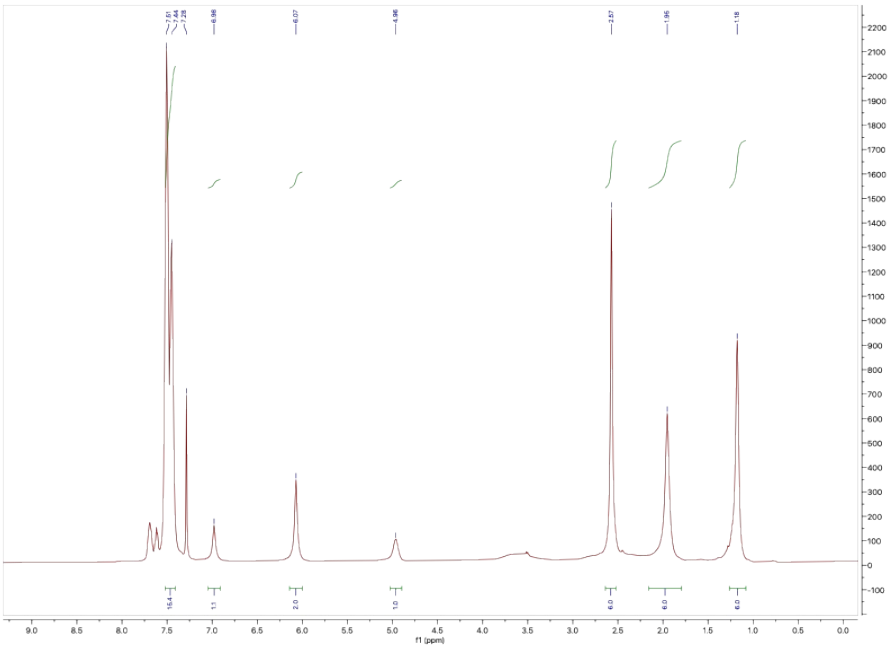

Figure S23. ^{1}H-NMR spectrum of [Cu(L^{2OiPr})(PPh_3)]PF_6 (**3**) in $CDCl_3$.

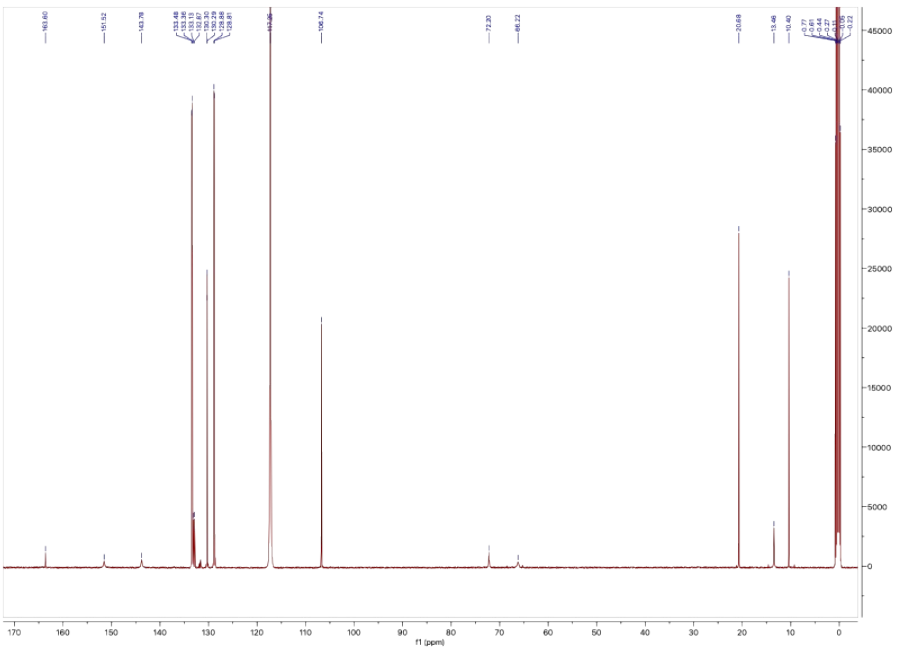

Figure S24. $^{13}C\{^{1}H\}$-NMR spectrum of [Cu(L^{2OiPr})(PPh_3)]PF_6 (**3**) in CD_3CN.

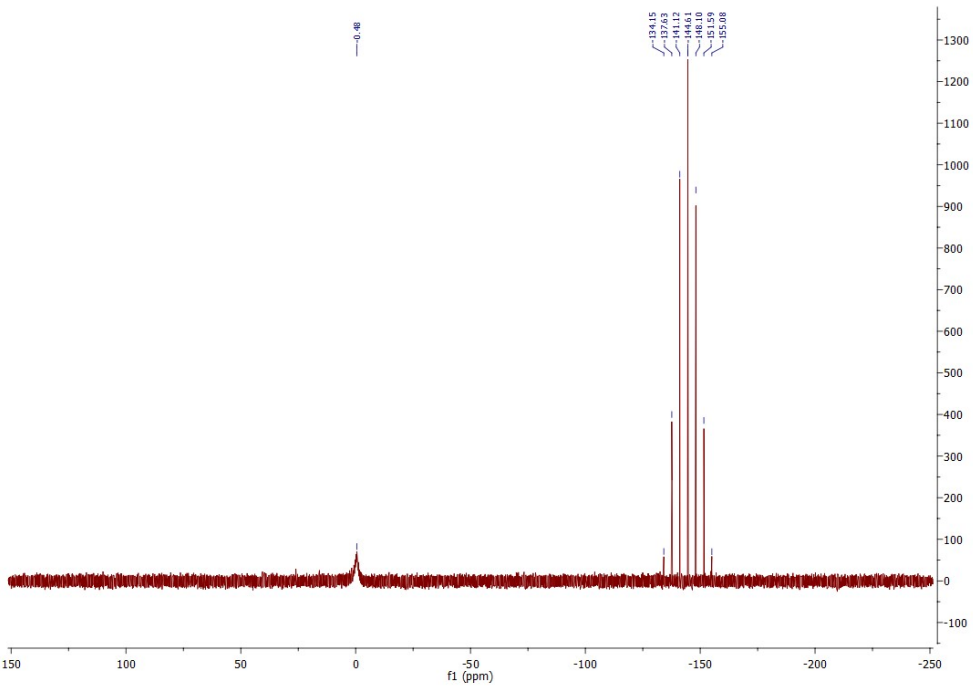

Figure S25. $^{31}P\{^{1}H\}$-NMR spectrum of $[Cu(L^{2OiPr})(PPh_3)]PF_6$ (**3**) in CD_3CN at 293K.

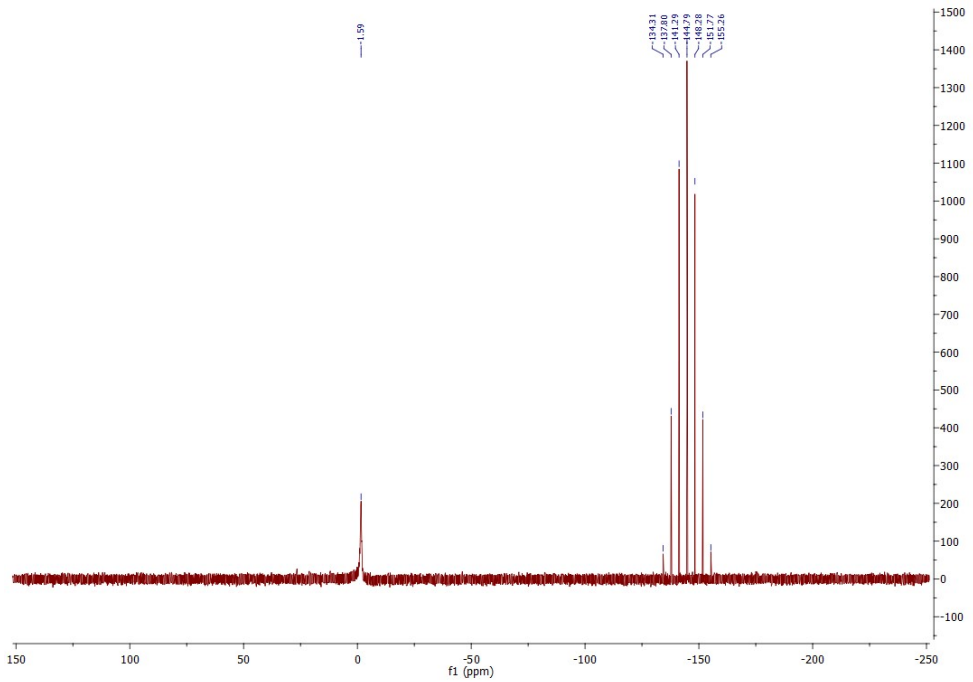

Figure S26. $^{31}P\{^{1}H\}$-NMR spectrum of $[Cu(L^{2OiPr})(PPh_3)]PF_6$ (**3**) in CD_3CN at 243K.

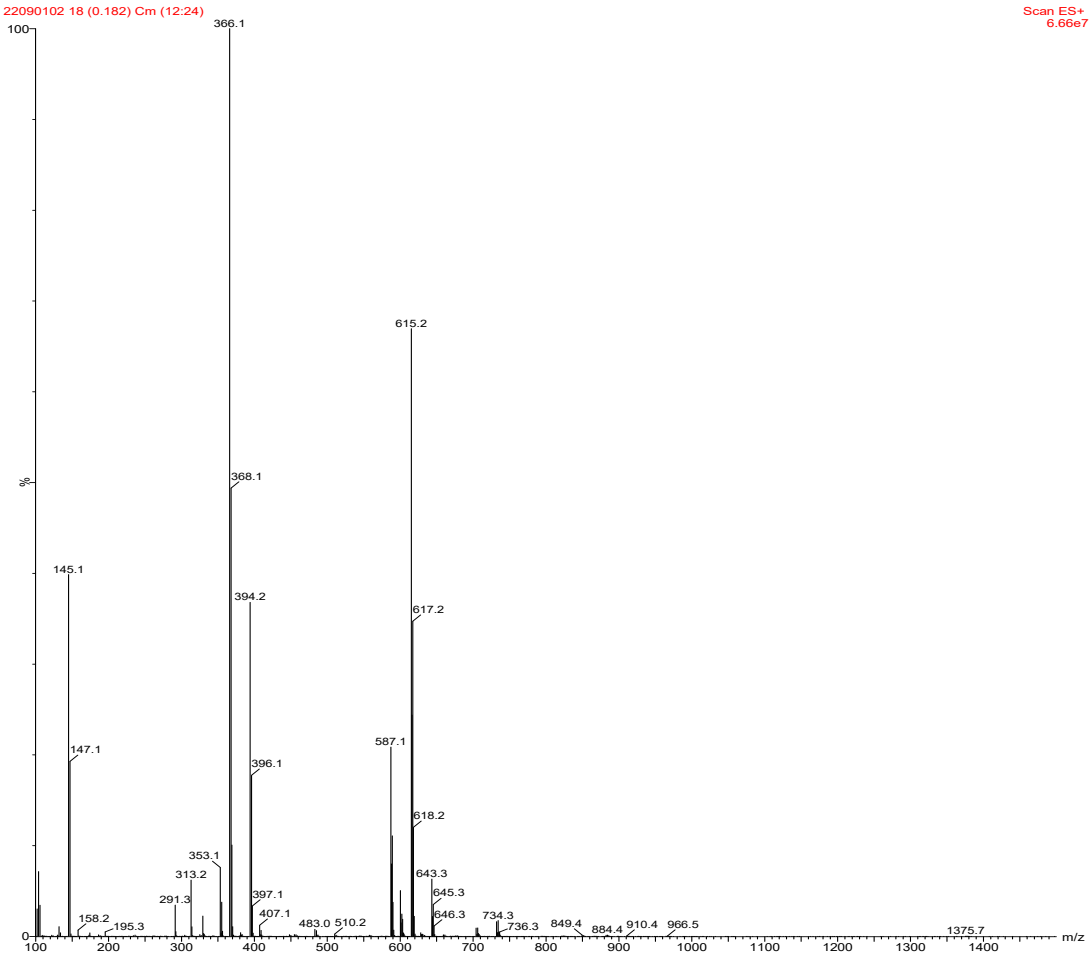

Figure S27. ESI-MS(+) spectrum of $[Cu(L^{2OiPr})(PPh_3)]PF_6$ (**3**).

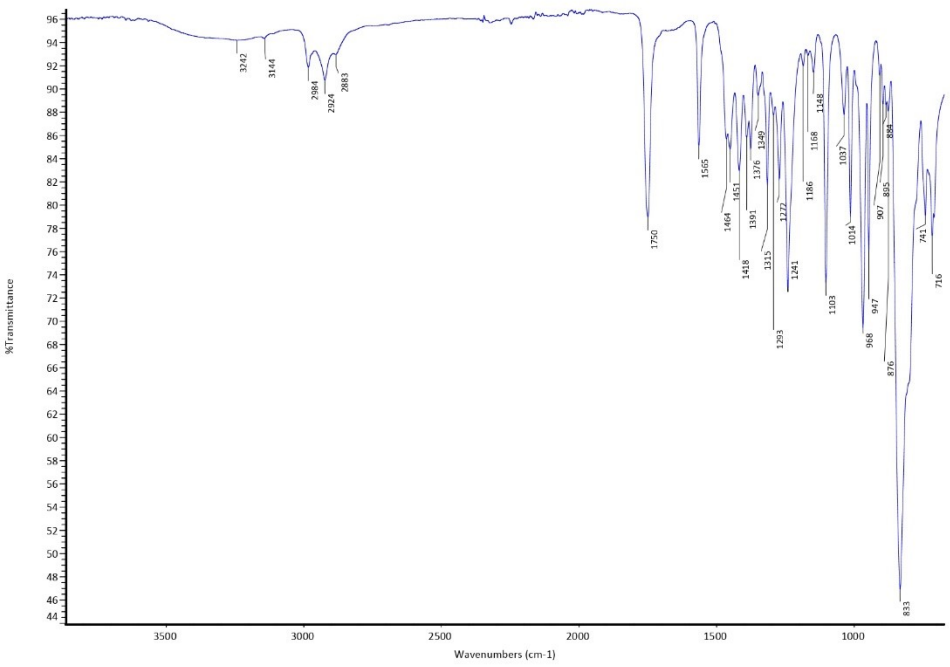

Figure S28. FT-IR spectrum of $[Cu(L^{2OiPr})(PTA)]PF_6$ (**4**).

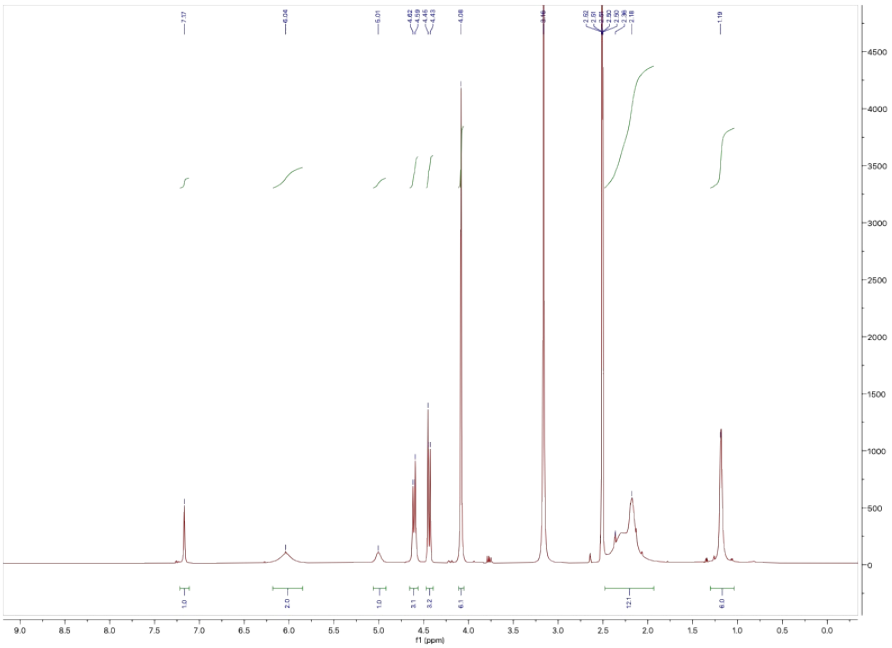

Figure S29. ^{1}H-NMR spectrum of [Cu(L^{2OiPr})(PTA)]PF$_6$ (**4**) in DMSO-d$_6$.

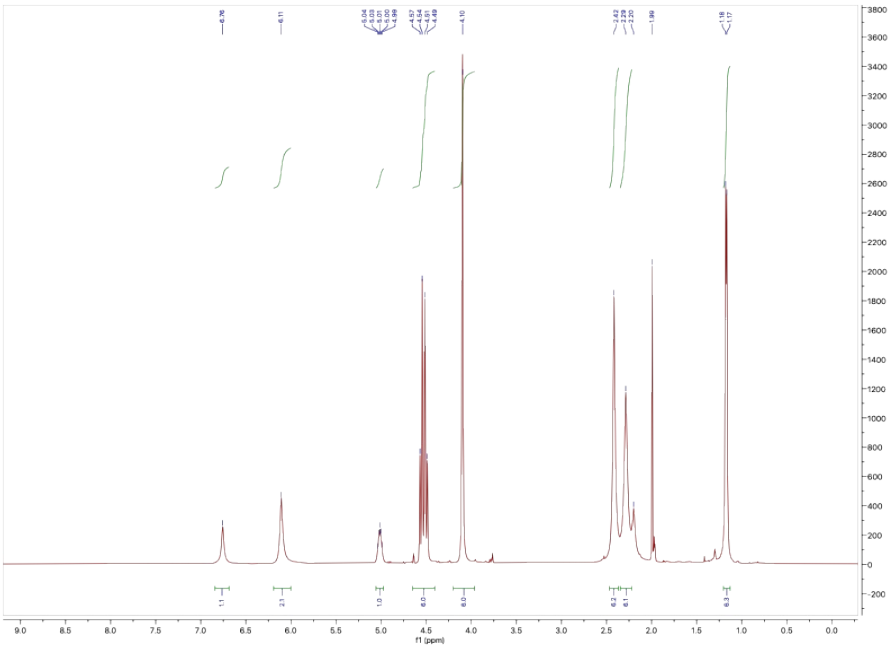

Figure S30. ^{1}H-NMR spectrum of [Cu(L^{2OiPr})(PTA)]PF$_6$ (**4**) in CD$_3$CN.

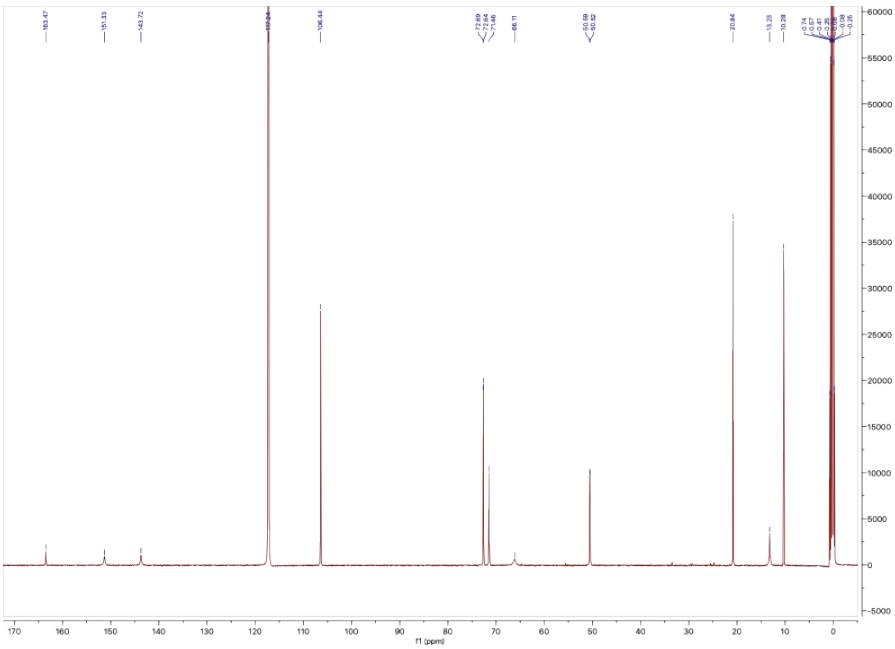

Figure S31. $^{13}C\{^{1}H\}$-NMR spectrum of $[Cu(L^{2OiPr})(PTA)]PF_6$ (**4**) in CD_3CN.

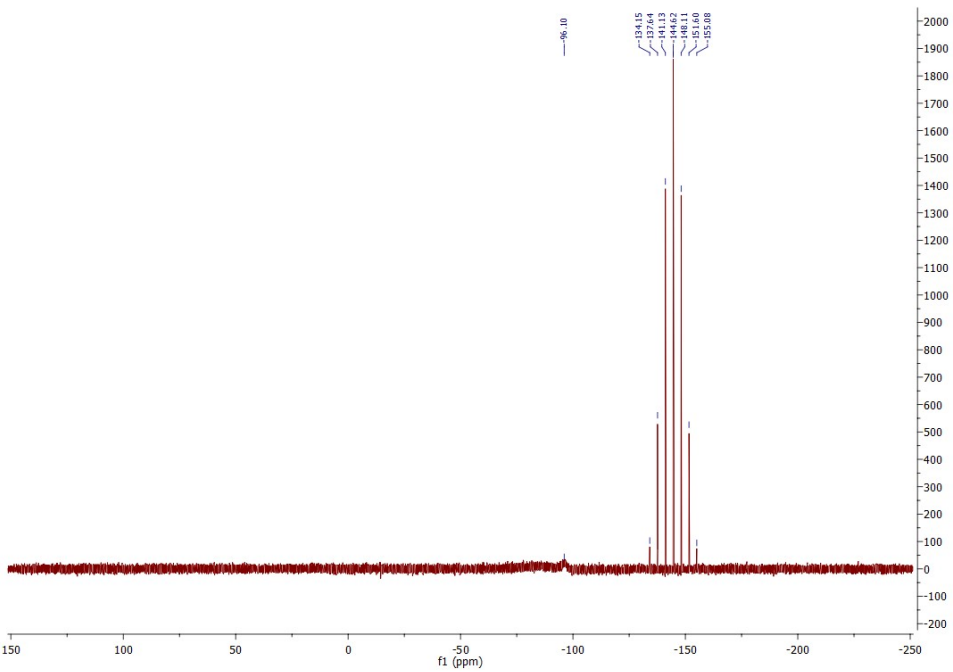

Figure S32. $^{31}P\{^{1}H\}$-NMR spectrum of $[Cu(L^{2OiPr})(PTA)]PF_6$ (**4**) in CD_3CN at 293K.

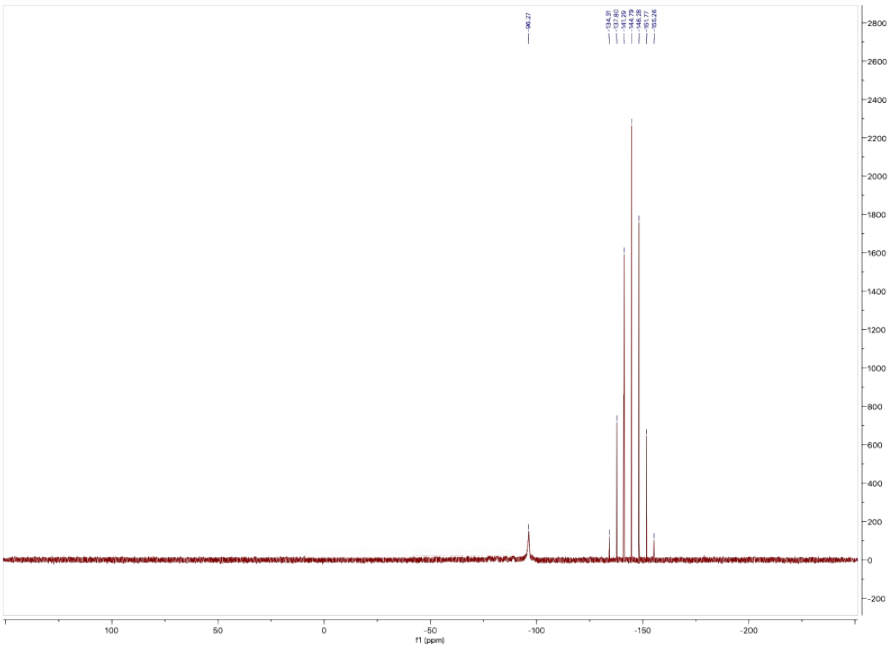

Figure S33. $^{31}P\{^{1}H\}$-NMR spectrum of $[Cu(L^{2OiPr})(PTA)]PF_6$ (**4**) in CD_3CN at 243K.

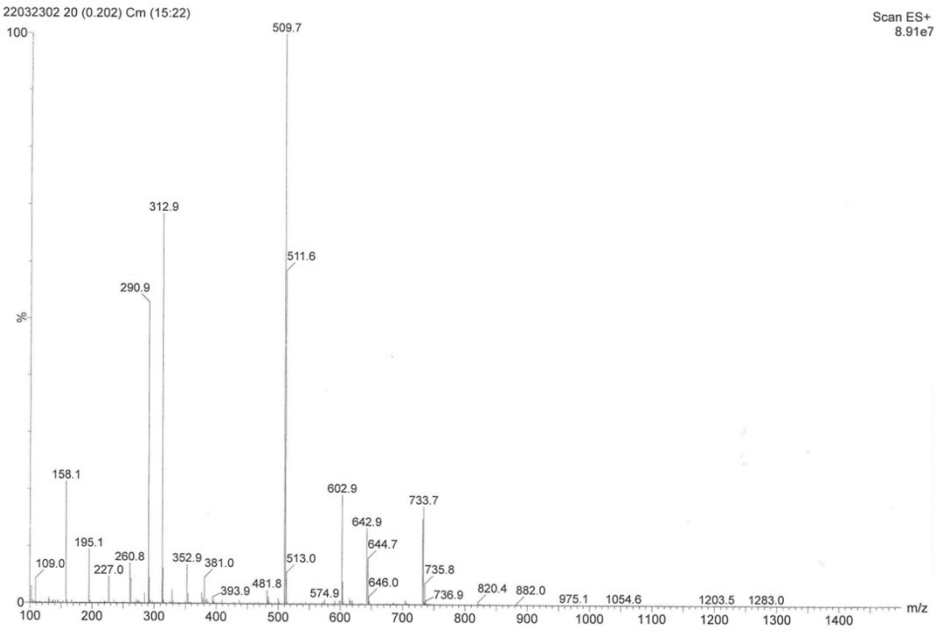

Figure S34. ESI-MS(+) spectrum in CH_3CN of $[Cu(L^{2OiPr})(PTA)]PF_6$ (**4**).

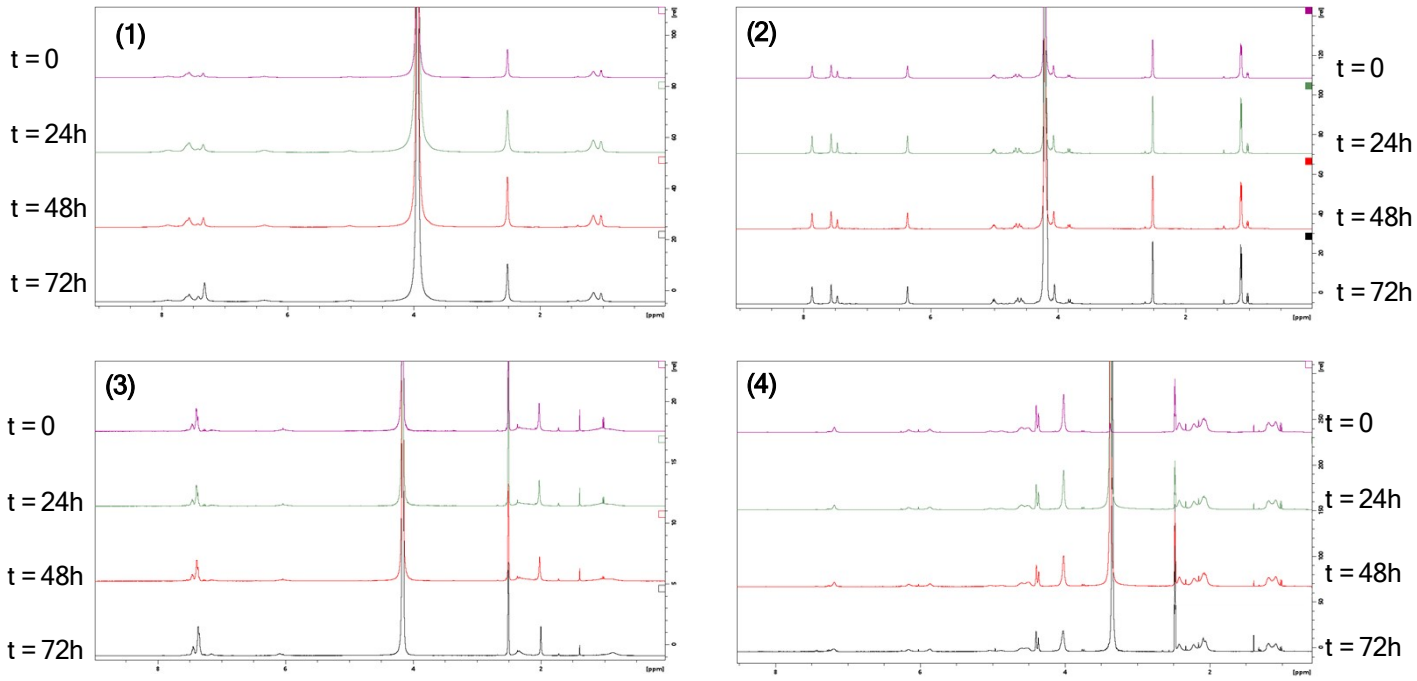

Figure S35. Stability Studies. The stability of the new complexes **1-4** in 0.5% DMSO/saline solution was also evaluated by using ^{1}H-NMR.

Table S1. XPS data (BE, FWHM, experimental and theoretical atomic ratios and proposed assignments) collected on complex (**3**).

Sample	Signal	BE (eV)	FWHM (eV)	atomic ratios (exp.)	atomic ratios (theor.)	Assignment
(**3**)	C1s	284.70	1.6	11.3	26	C-C + C-P (C1)
		286.0	1.6	4.3	5	C-N (C2)
		287.6	1.6	1.2	1	C-O (C3) + imp.
		288.6	1.6	1	1	COOR (C4) + imp
	N1s	400.7	2.6	N/Cu_tot = 4.4	N/Cu_tot = 4	N-C amine-like
	$P2p_{3/2}$	132.2	3.8			P-C P Ph_3 (P1)
		136.4	4.6			P-F PF_6 (P2)
	F1s	685.9	2.2			F-P PF_6
	$Cu2p_{3/2}$	932.8	2.5	1	1	Cu(I) complex
		935.3	2.5	0.1	0	Cu(II) $Cu(OH)_2$
	O1s	531.6	1.80	1.7	1	O=C (+ impurities)
		532.5	1.80	1	1	O-C
		534.1	1.80			physisorbed H_2O